



Contents lists available at ScienceDirect

Bioorganic & Medicinal Chemistry Letters

journal homepage: www.elsevier.com/locate/bmcl

Structure based design of nicotinamide phosphoribosyltransferase (NAMPT) inhibitors from a phenotypic screen

Daniel S. Palacios^{a,*}, Erik Meredith^a, Toshio Kawanami^a, Christopher Adams^a, Xin Chen^a, Veronique Darsigny^a, Erin Geno^a, Mark Palermo^a, Daniel Baird^b, Geoffrey Boynton^b, Scott A. Busby^b, Elizabeth L. George^b, Chantale Guy^b, Jeffrey Hewett^b, Laryssa Tierney^b, Sachin Thigale^b, Wilhelm Weihofen^b, Louis Wang^b, Nicole White^b, Ming Yin^b, Upendra A. Argikar^c

^a Global Discovery Chemistry, Novartis Institute for Biomedical Research, 22 Windsor Street, Cambridge, MA 02139, USA

^b Chemical Biology and Therapeutics, Novartis Institute for Biomedical Research, 181 Massachusetts Avenue, Cambridge, MA 02139, USA

^c PK Sciences, Novartis Institute for Biomedical Research, 250 Massachusetts Avenue, Cambridge, MA 02139, USA

ARTICLE INFO

Article history:

Received 17 October 2017

Revised 13 December 2017

Accepted 16 December 2017

Available online xxx

Keywords:

NAMPT

In silico screen

Structure based drug design

Cyclopropane

Nicotinamide phosphoribosyltransferase

ABSTRACT

Nicotinamide phosphoribosyltransferase is a key metabolic enzyme that is a potential target for oncology. Utilizing publicly available crystal structures of NAMPT and *in silico* docking of our internal compound library, a NAMPT inhibitor, **1**, obtained from a phenotypic screening effort was replaced with a more synthetically tractable scaffold. This compound then provided an excellent foundation for further optimization using crystallography driven structure based drug design. From this approach, two key motifs were identified, the (*S,S*) cyclopropyl carboxamide and the (*S*)-1-*N*-phenylethylamide that endowed compounds with excellent cell based potency. As exemplified by compound **27e** such compounds could be useful tools to explore NAMPT biology *in vivo*.

© 2017 Elsevier Ltd. All rights reserved.

Regulation of nicotinamide adenine dinucleotide (NAD⁺) levels within cells is critical given the importance of NAD⁺ in both maintaining cellular energy homeostasis and its role as an enzymatic cofactor.¹ There are multiple mechanisms within eukaryotic cells to sustain cellular NAD⁺ levels but the rate determining source is the conversion of nicotinamide (NAM) to nicotinamide mononucleotide (NMN) by the enzyme nicotinamide phosphoribosyltransferase (NAMPT). The NMN produced by NAMPT is then further processed to NAD⁺ by the enzyme Nicotinamide mononucleotide adenylyltransferase (NMNAT, Fig. 1A).² Several reports have demonstrated that cancerous cells express higher levels of NAMPT and have a higher NAD⁺ demand than normal cells.³ This evidence therefore suggests that blocking NAD⁺ production through the inhibition of NAMPT enzymatic activity could be selectively lethal to cancerous cells and consequently provide a therapeutic benefit.⁴

Recently, we disclosed the pyrrolo-pyrimidine NAMPT inhibitor **1** (Fig. 1B), which was discovered through a phenotypic screening campaign.⁵ While **1** is very potent in an A2780 Cell-Titer Glo™ (CTG) assay (IC₅₀: 6 nM) the construction of the pyrrolo-pyrimidine core requires a significant investment of synthetic effort.⁶

Given the structures of known NAMPT inhibitors,⁷ we hypothesized that this complex core is not necessary for NAMPT activity and we could identify an alternative to **1** that was more synthetically tractable and therefore more amenable to iterative optimization. In this vein, we used the crystal structure of NAMPT/FK866 (PDB code: 2GVJ)⁸ as the template for an *in silico* screen for alternative chemical matter. The pyridine of FK866 is in a pi-stacking position between Tyr18' and Phe193 which mimics the position of the natural ligand NMN to competitively inhibit enzyme function. Docking **1** into this pocket suggested that the pyridine nitrogen could form the same hydrogen-bond with the phenol of Tyr18 as observed for the analogous nitrogen in the FK866 crystal structure. To potentially enhance this interaction, a 2-aminopyridine was selected as a new head group because of the enhanced basicity of this pyridine nitrogen relative to an unsubstituted pyridine. The 2-aminopyridine was then used as the substructure search query to filter our internal compound collection, followed by docking into the FK866 binding pocket. A dozen top-scoring docking hits were selected and submitted for biological activity testing in the A2780 CTG assay. From this effort, the most promising ligand identified was 2-aminopyridine **2**, which we found to be equipotent to **1** in both the A2780 and CORL23 CTG assays.⁹ Furthermore, the cellular activity of **2** was rescued by concurrent treatment with 100

* Corresponding author.

E-mail address: daniel.palacios@novartis.com (D.S. Palacios).

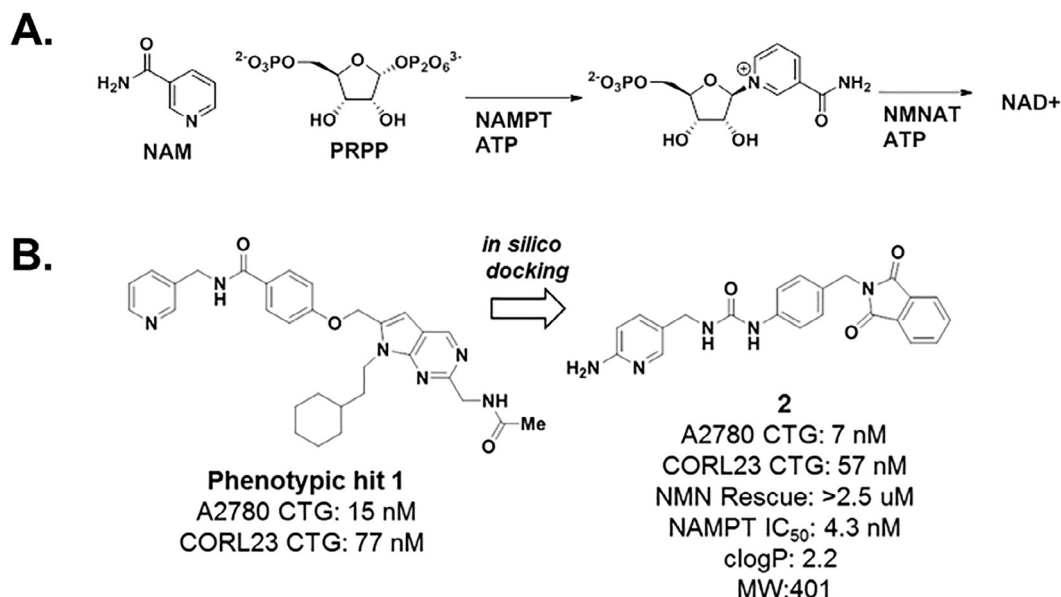


Fig. 1. Identification of cyclopropyl carboxamide NAMPT inhibitors from phenotypic hit **1**. A. NAMPT converts NAM to NMN on the path to NAD⁺. B. Structure of phenotypic hit **1** and *in silico* derived **2**.

μM of the NAMPT product NMN. Compound **2** was also found to inhibit NAMPT in a biochemical assay (Fig. 1B). This data strongly supports the conclusion that **2** is decreasing the viability of A2780 and CORL23 cells through direct inhibition of NAMPT. In addition to the potent activity of **2**, this small molecule has promising physicochemical properties (clogP: 2.2, MW: 401) and can be readily synthesized in a convergent fashion. Thus, **2** appeared to be a promising foundation to build a lead optimization campaign.

Examining the structure of **2**, we initially sought to explore the structure activity relationship (SAR) of the urea motif. We hypothesized that replacing the urea functionality could potentially improve the aqueous solubility and membrane permeability of the scaffold by decreasing the number of NH bonds. Furthermore, given the α,β unsaturated amide in FK866¹⁰ and the bicyclic NAM mimetics that are known in the literature,^{11,12} we postulated that the benzylic urea nitrogen was not engaged in a direct interaction with the target protein and could be replaced. As shown in Table 1 we first removed the aniline on the 2 position of the pyridine to simplify analog synthesis and found that pyridine **3** was approximately ten fold less potent in the A2780 CTG assay.¹³

Next, deleting the benzylic nitrogen gave amide **4**, which was a potent NAMPT inhibitor (IC₅₀: 25 nM) but was inactive in the CORL23 CTG assay. This type of disconnect between biochemical and cell based assays has also been reported for other NAMPT inhibitors.¹¹ We suspected that the increased flexibility of the ethyl bridge in **4** led to its greatly attenuated activity and we therefore rigidified the system by introducing unsaturation to give amide **5**. However, we were surprised to find that α,β unsaturated amide **5** was only moderately active with an IC₅₀ of 2000 nM in the CORL23 CTG assay. To further explore conformational constraints at this position, we utilized the Corey–Chaykovsky¹⁴ reaction to synthesize cyclopropyl carboxamide **6** and separated the two *trans* cyclopropane enantiomers. Upon testing, we found the (*S,S*) enantiomer afforded significantly improved activity over the parent urea **3**. We also found that the cellular activity of the cyclopropane motif is highly stereoselective as the corresponding (*R,R*) enantiomer **7** was inactive in both the A2780 and CORL23 CTG assays. Confirmation that NAMPT is the target of **6** was achieved through demonstration of the biochemical inhibition of NAMPT (Table 1). Though 3-pyridine cyclopropyl carboxamide NAMPT inhibitors

have been previously reported in the literature,¹⁵ this effort was limited to a phenylsulfone core. With this in mind, we were intrigued by the potential of the phthalimide moiety to provide new directions for the optimization of **6**.

The absolute configuration of the cyclopropane was determined through co-crystallization with NAMPT, as shown in Fig. 2. In addition to determining the absolute stereochemistry, the crystal structure also suggests the basis for the enhanced cellular activity of the

Table 1
SAR of the amide linker.

Cmpd	R	A2780 CTG (nM)	CORL23 CTG (nM)	NAMPT IC ₅₀ (nM)
3		100	NT ^a	3.1
4		>10,000	>10,000	25
5		NT	2000	10
6		27	35	<1
7		>2500	>10,000	>2500

^a Not tested.

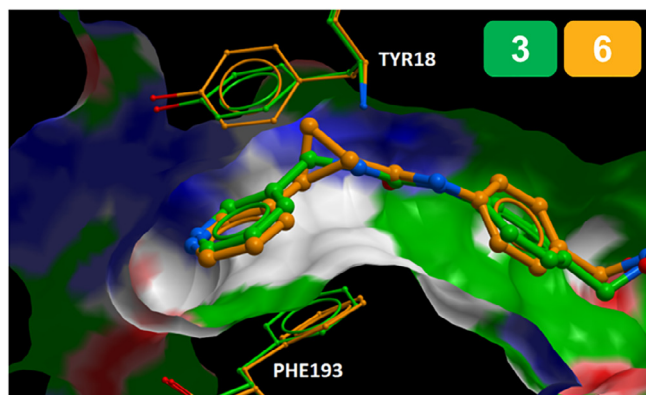


Fig. 2. Overlay of urea **3** (PDB:) and cyclopropane **6** (PDB:) in the NAMPT crystal structure showing the similar position of the pyridine nitrogen.

(*S,S*) cyclopropane relative to the urea. As described by others, the heterocyclic warhead of cellularly active NAMPT inhibitors acts as a nicotinamide mimetic and is ribophosphorylated by the enzyme.¹⁶ The position of the pyridine nitrogen within the catalytic pocket is therefore critical for this substitution reaction to proceed.

Strikingly, as shown in **Fig. 2**, there is a high degree of structural overlap between the aromatic rings of urea **3** and cyclopropane **6** and the pyridine nitrogens for the two ligands are in almost the exact same position within the binding pocket. Presuming that the binding pose is related to the reactive conformation of the ligand, we postulate that the cyclopropane preconfigures the position of the pyridine nitrogen into this conformation and therefore

Table 2
Combining the (*S*)-*N*-1-phenylethylamine and (*S,S*) cyclopropane.

Cmpd	A2780 CTG (nM)	CORL23 CTG (nM)
8	22	92
9	8	137
10	8	8
11	630	>2500
12	12	6
13	340	1330
14	405	>2500
15	5	22

reduces the entropy of binding of the cyclopropane relative to the urea.¹⁷

Concurrent to the exploration of the urea, we were also probing the SAR of phthalimide region of **2**. Given our aim to identify *in vivo* active molecules we decided to drive the optimization with cell based activity. As mentioned above, urea **2** has very poor aqueous solubility (<0.005 mM). In order to improve the solubility, we took advantage of the flexible SAR of the phthalimide portion of the molecule and appended solubilizing groups to the scaffold as shown in **Fig. 3A** and **Table 2**.

As demonstrated by morpholine **8** and piperazine **9**, these groups are well tolerated and substantially improve upon the solubility of the parent compound (Solubility at pH 6.8 for **8** = 0.13 mM, **9** = >1 mM). When we obtained an X-ray co-crystal structure of piperazine **9** bound to NAMPT we observed a hydrophobic pocket located close to the benzyl methylene of the central phenyl ring (**Fig. 3C**). Hypothesizing that occupying this pocket with a hydrophobic group could increase compound affinity, we synthesized the two alpha substituted amides **10** and **11** and we found that filling this pocket with the (*S*)-*N*-1-phenylethylamine

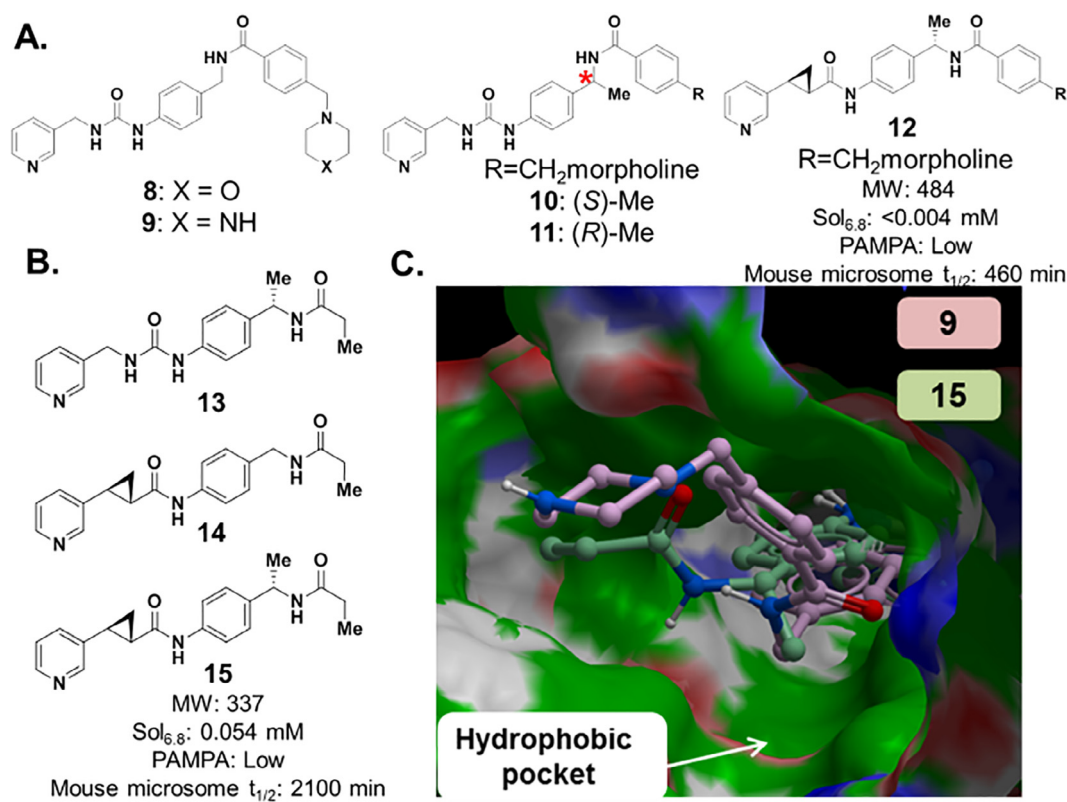


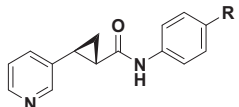
Fig. 3. The cyclopropane and (*S*)-benzyl amide enhance NAMPT potency. A. Combining the (*S*)-phenylethylamide and (*S,S*) cyclopropane does not effect potency on higher molecular weight NAMPT inhibitors. B. Combining the (*S,S*) cyclopropane and (*S*)-phenylethylamide on lower molecular weight compounds enabled the minimal pharmacophore **15**. C. Overlay of the co-crystal structure of **9** bound to NAMPT (PDB:) and **15** (PDB:).

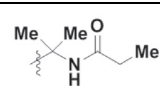
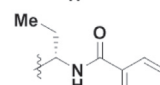
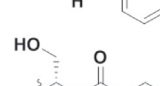
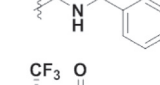
(compound **10**) significantly increases the activity of the scaffold in the CORL23 CTG assay. This interaction is also highly stereoselective as the corresponding (*R*)-*N*-1-phenylethylamide (compound **11**) is approximately 100 fold less active than the (*S*) enantiomer. Next, we were interested to discover if the combination of the (*S*, *S*)-cyclopropane and the (*S*)-*N*-1-phenylethylamide would further enhance cellular activity but we found, contrary to our expectation, that urea **10** and cyclopropane **12** are approximately equipotent.

While cyclopropane **12** displays excellent *in vitro* potency, we found **12** to have poor solubility, permeability and *in vitro* clearance. To address these poor properties, we set out to reduce the overall size and hydrophobicity of the molecule. However, as shown in Fig. 3B, both the (*S*)-*N*-1-phenylethylamide **13** and cyclopropane **14** were very weakly active in our cell based assays. Next, despite the equipotency of urea **10** and cyclopropane **12**, when we merged the analogous compounds **13** and **14** we were surprised to find that cyclopropane compound **15** gained greater than 50-fold potency in both the A2780 and CORL23 CTG assays versus the parent compounds. In addition, as we had hypothesized, the smaller ethylamide **15** is both more soluble and metabolically stable than benzyl morpholine **12**. Thus, ethylamide **15** revealed the utility of combining the cyclopropane and (*S*)-*N*-1-phenylethylamide to enable the installation of relatively small groups on the eastern portion of the molecule to improve compound properties. Furthermore, this result was achieved by challenging our assumption based on cyclopropane **12** that the (*S,S*) cyclopropane and (*S*)-*N*-1-phenylethylamide would not be additive in terms of compound activity. For our chemistry strategy, this was a lesson learned that SAR between closely related series may not always track and one has to always question preconceived wisdom regarding scaffold optimization.

Given the utility of the (*S*)-*N*-1-phenylethylamide, we next probed the SAR of this position to determine if the methyl group was ideal for activity and, as shown in Table 3, there is limited tolerance at this position with small non-polar groups being preferred. Even adding an additional carbon with ethyl **17** reduces the activity of the compound about tenfold relative to the methyl matched pair (compound **27e** Table 4). In addition, adding a polar atom, as demonstrated by primary alcohol **18**, deleteriously impacts the cell based activity of the scaffold (200 nM A2780 CTG).

Table 3
SAR of the (*S*) benzyl position.



Cmpd	R	A2780 CTG (nM)	CORL23 CTG (nM)
16		832	2310
17		43	137
18		200	630
19		1	4

Based on the SAR shown in Table 3, we decided to keep the methyl group fixed and commenced with an interrogation of the amide SAR. As shown in Scheme 1, the synthesis of these analogues began with the Heck reaction of 3-bromo pyridine **20** and *t*-butyl acrylate to give the alpha-beta unsaturated ester **21**. The *t*-butyl ester is critical because we found that the corresponding methyl ester was hydrolyzed during the Corey-Chaykovsky cyclopropanation and the resulting acid proved difficult to isolate. Deprotection of the ester with TFA followed by chiral chromatography (see Supporting information for details) then afforded enantiomerically pure **23**. Through this sequence, we were able to generate multi-gram quantities of the key non-racemic intermediate **23** in significantly fewer steps than was previously reported.¹⁴ Diversification of the amide began with the commercially available secondary amine **24** which was coupled to a range of acids using standard amide bond forming conditions. Reduction of the aryl nitro group then afforded the corresponding anilines **26a–i** and the ultimate step was a second amide bond formation to give compounds **27a–i**.

As shown in Table 4, the eastern amide was broadly tolerant of diverse substructures, enabling the identification of a number of potent compounds with diverse physicochemical properties. Aliphatic heterocycles such as tetrahydropyran **27b** and *N*-methyl proline **27d** have single digit nanomolar potency and good solubility. In addition, *N*-methyl proline **27d** shows an improved permeability profile, likely due to the formation of an intramolecular hydrogen bond between the amide proton and the proline nitrogen.¹⁸ An unsubstituted phenyl group was active and though the *in vitro* clearance was increased, this could be attenuated through the addition of electron withdrawing groups to the four position of the ring, as demonstrated by fluorine **27f** and nitrile **27g**.

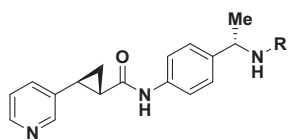
In addition, heterocycles such pyridine **27h** and pyrimidine **27i** can also replace the phenyl group with a small loss in activity but a significantly decreased *in vitro* clearance. Significantly, the CYP3A4 inhibition of these compounds is attenuated relative to previously reported cyclopropylcarboxamide NAMPT inhibitors¹⁴ (Table 4). This may in part be due to the potency combination of the cyclopropane and (*S*)-*N*-1-phenylethylamide which enables the installation of relatively small amide appendages.

Given the promising *in vitro* properties of phenyl amide **27e**, we decided to investigate the *in vivo* metabolic stability of this compound. As shown in Fig. S2 (supporting information), **27e** has good *in vivo* properties with a half-life of 90 min and a markedly reduced intrinsic clearance than was predicted by the mouse liver microsomes.

The good *in vivo* exposure of **27e** combined with its concise synthesis suggests that this small molecule would be an excellent tool to explore NAMPT biology both *in vivo* and *in vitro*. With this in mind, we employed a mouse CORL23 xenograft model and found that phenylamide **27e**, when dosed orally at 10 mg/kg bid, significantly reduced the growth of the implanted tumor (Fig. 4A). The antitumor efficacy that we observe for **27e** is comparable to the result shown in Fig. 4B for the known NAMPT inhibitor **28** (see Supporting information). Furthermore, we also found that the observed efficacy of **27e** correlates to the blockade of glycolytic flux, which requires NAD for turnover, as measured by the accumulation of the glycolysis intermediates fructose-6-phosphate and glucose-6-phosphate (Supporting information).¹⁹

To conclude, our pursuit of compounds that inhibit the function of the NAD⁺ producing enzyme NAMPT began with phenotypic screening hit **1**. The poor physicochemical properties and complex synthesis of pyrrolo-pyrimidine **1** catalyzed the search for alternative chemical matter and a consequent *in silico* screen identified 2-amino pyridine **2**. The promising cellular activity and much improved access to analogues of **2** enabled a structure based lead optimization effort to improve overall physicochemical properties.

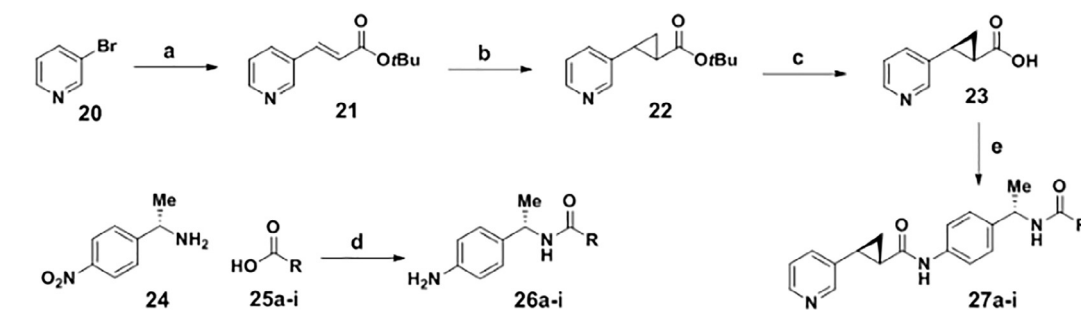
Table 4
SAR of the amide appendage.



Cmpd	R	A2780 CTG (nM)	CORL23 CTG (nM)	Sol _{pH6.8} (mM)	PERM class ^a	MLM $\mu\text{L min}^{-1} \text{mg}^{-1b}$	CYP3A4 (μM)
27a		5	18	0.041	L	83.7	4.2
27b		3	7	0.09	L	25.1	15.8
27c		30	111	0.52	L	43.2	9.4
27d		1	11	0.73	M	65.4	10.7
27e		1	8	<0.004	M	148	17.1
27f		2	12	0.006	M	13.7	4.7
27g		4	19	0.175	L	53	0.5
27h		14	46	0.01	H	<3.42	0.95
27i		14	17	0.027	M	38.4	7.2

^a Permeability class, based on PAMPA profiling.

^b Mouse liver microsome.



Scheme 1. Synthesis reagents and conditions. (a) *tert*-Butyl acrylate (1.5 eq), Pd(OAc)₂ (0.05 eq), tri-*o*-tolylphosphine (0.1 eq), DIPEA (1.5 eq), DMF, 110 °C, 72%; (b) trimethylsulfoxonium iodide (2.0 eq), sodium hydride (2 eq), DMSO, 50 °C, 95%; (c) TFA (6 eq), DCM, 23 °C; chiral separation, 45%; (d) carboxylic acid (1.05 eq) HATU (1.05 eq), DIPEA (3 eq), DMF, 23 °C; zinc (5 eq), ammonium chloride (5 eq), EtOH, water, 50 °C, 30 min, 91%, two steps; (e) **23** (1 eq) **26a-i** (1 eq) HATU (1.05 eq), DIPEA (4 eq), DMF, 23 °C, 65%.

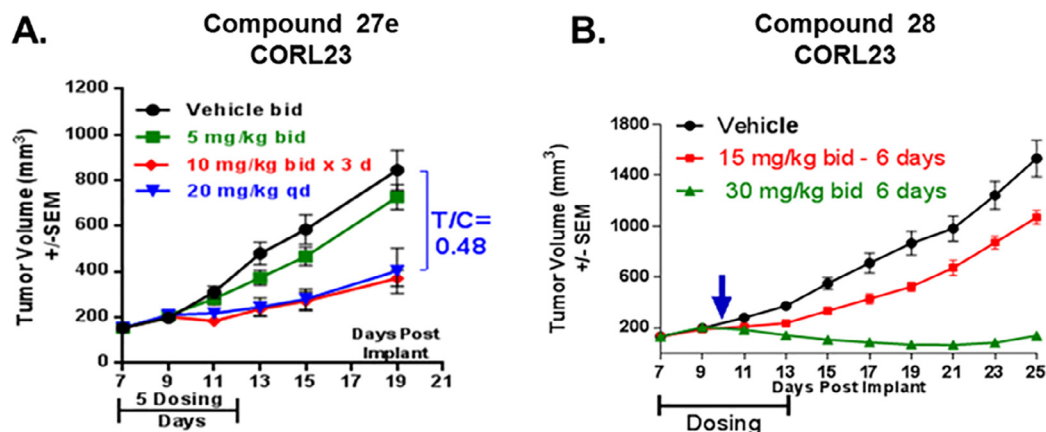


Fig. 4. *In vivo* activity in a CORL23 xenograft model. A. *In vivo* efficacy of **27e** dosed orally in a CORL23 xenograft. B. Efficacy data for the oral administration of compound **28**.

Two insights obtained from this work were the identification of the (*S,S*) cyclopropylcarboxamide and the (*S*)-*N*-1-phenylethylamide as key functional groups that enhance the activity of these NAMPT inhibitors. When combined, these two motifs can synergize to yield highly ligand efficient inhibitors, as exemplified by ethylamide **15**. The cellular potency of the cyclopropyl carboxamides tolerates a broad range of structures in the eastern portion of the molecule, which can be utilized to tune compound properties or to potentially generate probe compounds to interrogate NAMPT biology. These optimization efforts culminated in phenyl amide **27e**, a compound with excellent *in vivo* characteristics that was efficacious in a CORL23 mouse xenograft experiment.

Acknowledgments

We thank the GDC separations group for the asymmetric purifications and Frank Cook in Analytical Sciences for Fig. S4. This research was funded by the Novartis Institutes for Biomedical Research.

A. Supplementary data

Supplementary data (experimental details, representative curves for the biochemical inhibition of NAMPT, pharmacokinetic and pharmacodynamic data of the compounds) associated with this article can be found, in the online version, at <https://doi.org/10.1016/j.bmcl.2017.12.037>.

References

- Cantó C, Menzies KJ, Auwerx J. *Cell Metab.* 2015;22:31–53.
- Revollo JR, Grimm AA, Imai S. *J Biol Chem.* 2004;279:50754–50763.
- (a) Wang B, Hasan MK, Alavarado E, Yuan H, Wu H, Chen WY. *Oncogene.* 2011;30:907–921;
(b) Bi T-Q, Che X-M, Liao X-H, et al. *Oncol Rep.* 2011;26:1251–1257;
(c) Shackleford RE, Bui MM, Coppola D, Hakam A. *Int J Clin Exp Med.* 2010;3:522–527;
(d) Maldí E, Travelli C, Caldarelli A, et al. *Pigm Cell Melanoma Res.* 2013;26:144–146.
- (a) Hasmann M, Schemainda I. *Cancer Res.* 2003;63:7436–7442;
(b) Chiarugi A, Dölle C, Felizi R, Ziegler M. *Nature Rev. Cancer.* 2012;12:741–752.
- Estoppey D, Hewett J, Guy CT, et al. *Sci Rep.* 2017;7:42728.
- Irie O, Ehara T, Iwasaki A, et al. *Bioorg Med Chem Lett.* 2008;18:3959–3962.
- Galli U, Travelli C, Massarotti A, et al. *J Med Chem.* 2013;56:6279–6296.
- Khan JA, Tao X, Tong L. *Nat Struct Biol.* 2006;13:582–588.
- Gunzner-Toste J, Zhao G, Bauer P, et al. *Bioorg Med Chem Lett.* 2013;23:3531–3538.
- Hasmann M, Schemainda I. *Cancer Res.* 2003;63:7436–7442.
- Zheng X, Bauer P, Baumeister T, et al. *J Med Chem.* 2013;56:6413–6433.
- Dragovich PS, Bair KW, Baumeister T, et al. *Bioorg Med Chem Lett.* 2013;23:4875–4885.
- Zheng X, Bauer P, Baumeister T, et al. *J Med Chem.* 2013;56:4921–4937.
- Li JJ. *Named Reactions in Heterocyclic Chemistry.* 2nd ed. Hoboken, New Jersey: John Wiley & Sons; 2005.
- Giannetti AM, Zheng X, Skelton NJ, et al. *J Med Chem.* 2014;57:770–792.
- Oh A, Ho Y-C, Zak M, et al. *ChemBioChem.* 2014;15:1121–1130.
- Boström J, Grant A. In: Mannhold R, ed. *Exploiting Ligand Conformations in Drug Design*, Vol. 37. Weinheim, Germany: Wiley-VCH; 2007:183–205.
- Kuhn B, Mohr P, Stahl M. *J Med Chem.* 2010;53:2601–2611.
- Tan B, Young DA, Lu ZH, et al. *J Biol Chem.* 2013;288:3500–3511.